



Molecular Crystals and Liquid Crystals Science and Technology. Section A. Molecular Crystals and Liquid Crystals

Publication details, including instructions for authors and
subscription information:

<http://www.tandfonline.com/loi/gmcl19>

Neutron and Raman Scattering Studies of the Lattice and Methyl-Group Dynamics in Solid p-Xylene

J. Kalus^a, M. Monkenbusch^b, I. Natkaniec^{c,d}, M. Prager^b, J.
Wolfrum^a & F. Wörlén^a

^a Physikalisches Institut der Universität Bayreuth, 95440, Bayreuth,
FRG

^b Institut für Festkörperforschung der Kernforschungsanlage Jülich,
52425, Jülich, FRG

^c Frank Laboratory of Neutron Physics, JINR, 141980, Dubna, Russia

^d Institute of Nuclear Physics, 31-342, Krakow, Poland

Version of record first published: 24 Sep 2006.

To cite this article: J. Kalus, M. Monkenbusch, I. Natkaniec, M. Prager, J. Wolfrum & F. Wörlén
(1995): Neutron and Raman Scattering Studies of the Lattice and Methyl-Group Dynamics in Solid p-
Xylene, Molecular Crystals and Liquid Crystals Science and Technology. Section A. Molecular Crystals
and Liquid Crystals, 268:1, 1-20

To link to this article: <http://dx.doi.org/10.1080/10587259508030989>

PLEASE SCROLL DOWN FOR ARTICLE

Full terms and conditions of use: <http://www.tandfonline.com/page/terms-and-conditions>

This article may be used for research, teaching, and private study purposes. Any
substantial or systematic reproduction, redistribution, reselling, loan, sub-licensing,
systematic supply, or distribution in any form to anyone is expressly forbidden.

The publisher does not give any warranty express or implied or make any representation
that the contents will be complete or accurate or up to date. The accuracy of any
instructions, formulae, and drug doses should be independently verified with primary
sources. The publisher shall not be liable for any loss, actions, claims, proceedings,
demand, or costs or damages whatsoever or howsoever caused arising directly or
indirectly in connection with or arising out of the use of this material.

Neutron and Raman Scattering Studies of the Lattice and Methyl-Group Dynamics in Solid *p*-Xylene

J. KALUS¹, M. MONKENBUSCH², I. NATKANIEC^{3,*}, M. PRAGER²,
J. WOLFRUM¹, F. WÖRLEN¹

¹ *Physikalisches Institut der Universität Bayreuth, 95440 Bayreuth, FRG*

² *Institut für Festkörperforschung der Kernforschungsanlage Jülich, 52425 Jülich FRG*

³ *Frank Laboratory of Neutron Physics, JINR, 141980 Dubna, Russia*

(Received March 14, 1994; in final form June 6, 1994)

Solid $p\text{-C}_6\text{H}_4(\text{CH}_3)_2$ and $p\text{-C}_6\text{H}_4(\text{CD}_3)_2$ have been studied over a temperature range from 10 K up to the melting point of ~ 287 K by Raman- and Incoherent Inelastic Neutron-Scattering (IINS). The methyl torsion frequencies deduced from the Raman- and IINS-spectra are different because of the strong coupling of these modes with phonons and their dispersion in the Brillouin zone. A decrease in frequencies and a strong broadening, especially of the high frequency phonons where methyl torsions are predominant, have been observed in Raman- and IINS-spectra with increasing temperature. A lattice dynamics model based on the atom-atom potential set IVa of parameters given by Williams can, after some small modifications, satisfactorily explain the dynamics of a *p*-xylene crystal. Modified potential parameters better reproduce the experimental data and allow one to study the coupling of the internal methyl rotation with the lattice modes in more detail.

Keywords: *Lattice dynamics, molecular crystals*

INTRODUCTION

In the condensed state intermolecular forces play an important role in the internal rotation of a molecular group. The hindered methyl-group rotation about a single covalent bond provides a comparatively simple example of such internal motions occurring in many molecular systems and over a wide temperature range.¹ When the potential related to rotation is comparatively low, the internal rotation frequency corresponds in magnitude to the optical lattice mode frequencies and both can be coupled. In this case, complementary information obtained by several physical methods is necessary to get a comprehensive picture of the dynamics of the methyl group. Results of NMR, IINS, Raman (R) and infrared (IR) experiments on methyl dynamics in the solid state have recently been published (see references 2 and 3 and references therein).

The NMR measurements of the spin-lattice relaxation time in solid *p*-xylene⁴ point to two relaxation processes for the methyl groups with an activation energy of about

* Permanent address: Institute of Nuclear Physics, 31-342 Krakow, Poland.

2 kJ/mol below 33 K and of about 4 kJ/mol above this temperature. The activation energy for the molecular rotation observed at $T > 150$ K was found to be 16 kJ/mol. A recently re-examined spin-lattice relaxation time T_1 of *p*-xylene at low temperatures, different from the one previously obtained,⁵ has been explained by the fact that the temperature dependence of the tunnelling frequency and the random reorientation of the CH_3 groups with an activation energy of 4.5 kJ/mol was taken into account.

The IR results and Raman spectra experiments from liquid *p*-xylene⁶ appear to be consistent with the assumption of the almost free rotation of the methyl groups. Raman studies of solid *p*-xylenes⁷ during cooling to about 100 K show significant changes in the spectra with temperature and deuteration of the substance. By comparing the low frequency Raman spectra of *p*- $\text{C}_6\text{H}_4(\text{CH}_3)_2$, $\text{C}_6\text{H}_4(\text{CD}_3)_2$ and $\text{C}_6\text{D}_4(\text{CH}_3)_2$ samples at 93 K, the band at about 130 cm^{-1} was attributed to a symmetric libration of CH_3 groups. The frequencies at 155 and 120 cm^{-1} observed in the IR absorption of *p*- $\text{C}_6\text{H}_4(\text{CH}_3)_2$ and $\text{C}_6\text{H}_4(\text{CD}_3)_2$ at 93 K have been assigned to an antisymmetric libration of CH_3 and CD_3 groups, respectively. On the basis of the temperature behaviour of the Raman spectra a structural phase transition in the temperature range 170–200 K was suggested.⁸

X-ray studies of the crystal structure of protonated *p*-xylene⁹ show that there is no evidence for any phase transition in the temperature range from 110 K up to the melting point at 286 K. At 180 K the crystal structure is monoclinic: $\text{P2}_1/\text{n}$, $a = 0.5806(2)$, $b = 0.5023(1)$, $c = 1.1215(2)$ nm, $\beta = 100.48(2)^\circ$, $V = 0.32161(19)\text{ nm}^3$, $Z = 2$, $D = 1.096\text{ g/cm}^3$. The crystal packing scheme for *p*-xylene is given in Figure 1. This figure represents a view of the unit cell along the \bar{a} direction. Note, that four molecules in the

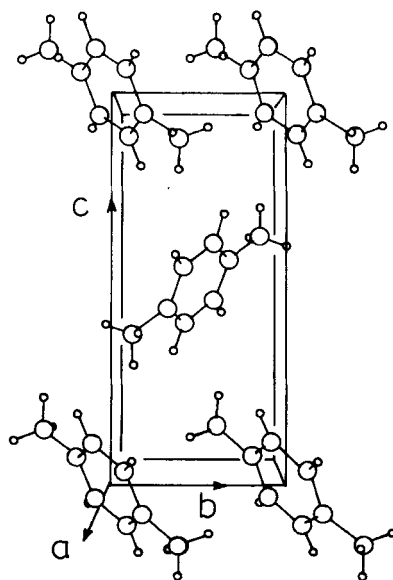


FIGURE 1 View of the unit cell of *p*-xylene along \bar{a} -direction. Notice that the four molecules on the back side of the cell are not shown.

back of this cell are not shown for the sake of convenience. The molecules are packed into chains along the \vec{b} direction via van der Waals contacts. The center of symmetry of the *p*-xylene molecule coincides with the space group center. Recent results of the high resolution neutron powder diffraction experiments¹⁰ confirm this structure down to the liquid helium temperature. The lattice parameters of deuterated *p*-xylene at 4 K are: $a = 0.57355(4)$, $b = 0.49504(1)$, $c = 1.11418(3)$ nm and $\beta = 100.71^\circ(2)$. In Figure 2 the temperature dependence of lattice parameters a , b , c and the unit cell volume are presented.

This paper reports on the measurements of the IINS-spectra of protonated and deuterated *p*-xylene. The IINS spectra from a solid $\text{C}_6\text{H}_4(\text{CH}_3)_2$ sample have also been studied with different resolutions over a wide temperature range from 10 K up to the melting point. Furthermore an accurate analysis of the Raman spectra of both protonated and deuterated samples in the temperature region from 15 to 280 K is presented. The lattice dynamics calculations with methyl rotation coupling are performed with a model based on a set of atom–atom potential parameters.¹¹ A good agreement with the structure and lattice frequencies of a benzene crystal was found with this set of parameters.¹² For a better fit to the experimental data of *p*-xylene some parameters of the atom–atom potentials were slightly modified.

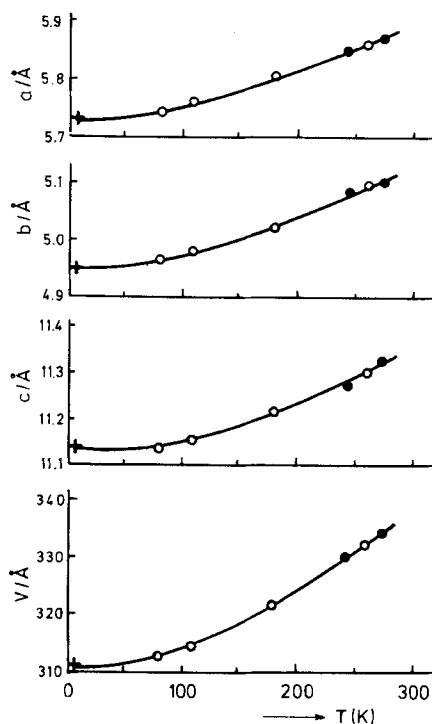


FIGURE 2 Unit-cell parameters and volume of *p*-xylene versus temperature. Combined results from X-ray powder data (●), single crystal measurements (○)⁹ and neutron powder data (+).¹⁰

EXPERIMENTAL DETAILS AND RESULTS

Commercial $p\text{-C}_6\text{H}_4(\text{CH}_3)_2$ and $p\text{-C}_6\text{H}_4(\text{CD}_3)_2$ were purchased from the Bayer company. The isotopic purity of deuterated methyl groups in the partially deuterated p -xylene compound was higher than 99.5%.

Inelastic neutron scattering experiments at 15 K were carried out with the SV22 time-of-flight spectrometer at the FRJ2 reactor of the KFA Jülich. The incident energy was 36.4 meV and the energy resolution of the elastic line was $\Delta E = 1.8$ meV. Powdered samples were contained in a rectangular cell 3×2 cm². The thickness of the cell was such that only 13% and 9% of the incident neutrons were scattered from the protonated and deuterated samples, respectively. The energy loss spectra have been summed over the scattering angles between 75° and 81°. Standard programs were used to transform the data to scattering law $S(Q, \omega)$ spectra, where $\hbar Q$ and $\hbar\omega$ are the momentum- and energy-transfer of the neutrons. The results shown in Figure 3 are not normalized and are given in different arbitrary units of $S(Q, \omega)$. The increase of $S(Q, \omega)$ at low ω -values stems from the influence of the elastic peak and from the $(1/\omega)$ factor in the scattering law.

In the frequency range below 250 cm⁻¹ five prominent maxima, marked 1 to 5 in Figure 3, were observed. The energies of these peaks are given in Table 1. It is quite evident that peak 3, which is very intense for protonated p -xylene and relatively low in intensity for deuterated p -xylene is related to the internal rotation of the methyl-groups. The reduction in energy when going from protonated to deuterated p -xylene can be understood qualitatively as being due to the increase of mass and moment of

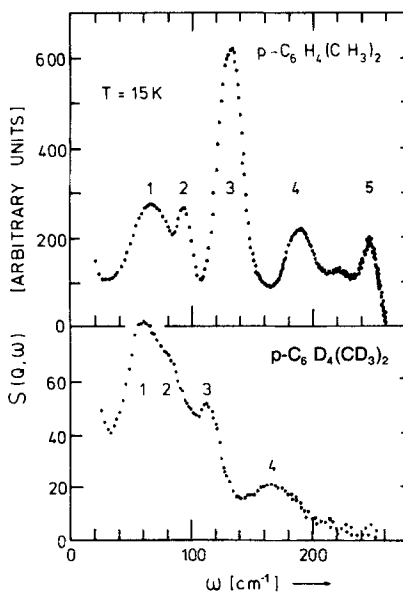


FIGURE 3 The scattering law $S(Q, \omega)$ at $T = 15$ K for protonated (upper part) and deuterated (lower part) p -xylene as measured with the SV 22 spectrometer at the FRJ2 at the KFA, Jülich. The numbers 1 to 5 indicate prominent peaks in the spectra.

TABLE I

Peak positions in the density of states of protonated and deuterated *p*-xylene as extracted from Figure 3 and 4. The energies are in cm^{-1} . The numbering of the peaks is indicated in the figures. The 15 K measurements were carried out at the SV 22 spectrometer. The 10 and 80 K measurements were carried out at the NERA spectrometer and the 85, 155 and 235 K measurements at the KDSOG-M spectrometer

No.	$p\text{-C}_6\text{D}_4(\text{CD}_3)_2$	$p\text{-C}_6\text{H}_4(\text{CH})_2$					
	15 K	15 K	10 K	80 K	85 K	155 K	235 K
1	61	65	66	67	67	63	60
2	81	93	92	91	93	90	85
3	113	132	130	123	125	115	105
4	170	186	184	181	183	180	—
5	—	244	243	235	235	—	—
6	—	—	296	296	296	—	—
7	—	—	325	325	—	—	—

inertia. This will be explained in more detail on the basis of a model calculation of lattice dynamics presented in the chapter devoted to the lattice dynamics. It was found in reference ³ that peak 3 in protonated *p*-xylene is a doublet.

The temperature dependence of the protonated *p*-xylene IINS-spectrum was measured at the IBR-2 high-flux pulsed reactor of JINR, Dubna, using the KDSOG-M and NERA time-of-flight inverted geometry spectrometers.^{13,14} The incident neutron energies were determined by measuring the neutron time-of-flight along the reactor-to-sample distance of 29.7 m and 109.5 m, respectively. The scattered neutron energy is fixed by the pyrolytic graphite analyzers ($E_f = 4.7$ meV and $\Delta E_f \approx 0.6$ meV, respectively) mounted behind beryllium filters. The resolution of the KDSOG-M spectrometer is about 5–7% in the frequency range of 100–500 cm^{-1} , while the resolution of the NERA spectrometer is roughly 3 times better, i.e. about 2%. The sample (approx. 10 cm^3) in a rectangular cell 16×16 cm^2 , was placed in a cryostat cooled by liquid helium or nitrogen. The time-of-flight IINS-spectra measured at different scattering angles from 30° to 150° were summed and transformed to the amplitude weighted phonon density of states spectra $G(\omega)$, using the one-phonon scattering formula.¹⁵ These transformed spectra at 10 K and 80 K are shown in Figure 4 in the frequency range up to 350 cm^{-1} . The temperature dependence of $G(\omega)$ measured with the KDSOG spectrometer in the temperature range of 85–275 K were published in reference.¹⁶ At low temperatures and below 350 cm^{-1} seven prominent maxima are seen in the $G(\omega)$ functions. Their energies are given in Table 1.

The first broad maximum at an average energy of about 65 cm^{-1} does not depend significantly on deuteration of the methyl group or temperature. So, it should correspond mainly to translational lattice vibrations and librations around the direction perpendicular to the plane of the benzene ring. It seems that these modes are not strongly coupled with the methyl rotation.

Peak 2 should correspond to the intermolecular libration modes. Its energy corresponds well with a strong Raman doublet seen in Figure 5a at about 90 cm^{-1} . This band shifts only slightly with increasing temperature.

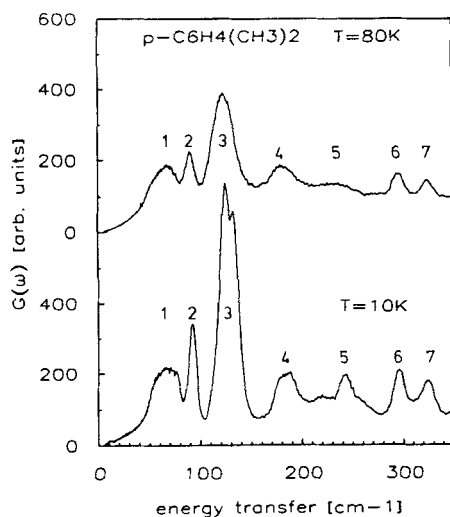


FIGURE 4 Temperature dependence of the amplitude weighted phonon density of states $G(\omega)$ of protonated *p*-xylene at 10 and 80 K as measured with the NERA spectrometer at the IBR-2 pulsed reactor at JINR, Dubna. The numbers indicate prominent peaks in the spectra and their energies are given in Table 1.

Peak 3 is very intense and shows a doublet structure at low temperature. With increasing temperature the width of this peak becomes significantly broader. The decrease of energy as a function of temperature of this peak is much stronger than was found for all other maxima in the general density of states function (see also reference).¹⁶ The strongly anharmonic behaviour of this peak is additional experimental evidence of hindered rotations of CH_3 groups caused by the intermolecular potential. The energy of this peak corresponds to four Raman lines at 111, 121, 137.5 and 143 cm^{-1} . As we will see in the model calculations, two infrared-active modes also have energies in this region. All modes show large librational amplitudes in the calculations.

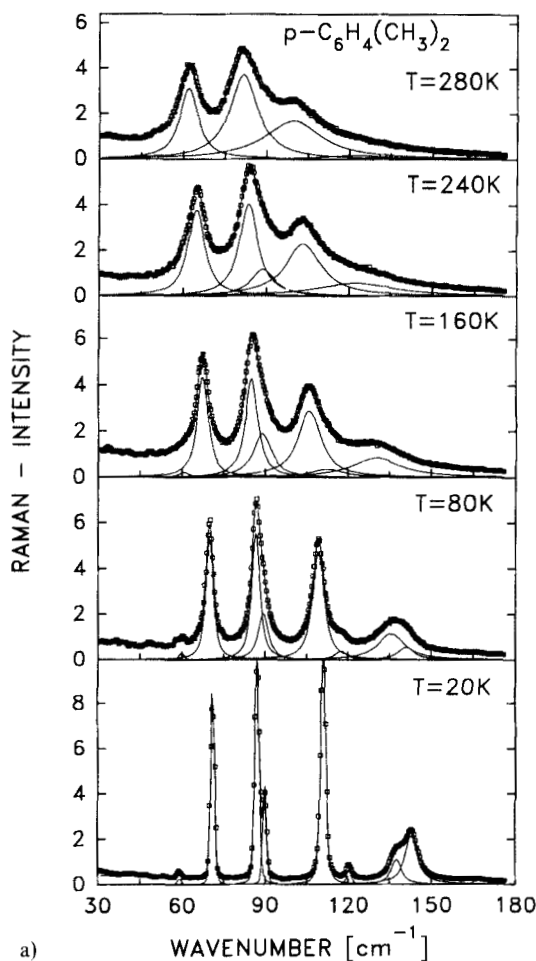
Peak 4, according to IR assignment,⁷ should correspond to the $\gamma(\text{C-methyl})$ internal vibration. The width of 20 cm^{-1} at 10 K evidences the dispersion of this mode, which might be an indication of a coupling with methyl rotations.

Peak 5 is well seen at liquid helium temperature for protonated *p*-xylene, only. One can see in Figure 3 that it disappears in the deuterated substance $p\text{-C}_6\text{D}_4(\text{CD}_3)_2$ and is strongly broadened (see Figure 4) at liquid nitrogen temperature for $p\text{-C}_6\text{H}_4(\text{CH}_3)_2$. This anharmonic behaviour allows one to assign this peak as the second rotational excitation of the CH_3 groups. The energy of peak 5, which is $E_{02} = 243 \text{ cm}^{-1}$, is lower than twice the average energy of peak 3. Peak 3 was identified as coming mainly from the first rotational excitation of the CH_3 groups, with a mean energy of $E_{01} = 130 \text{ cm}^{-1}$.

Peak 6 is seen by IR spectroscopy at 298 cm^{-1} and peak 7 by Raman spectroscopy at 316 cm^{-1} . They are assigned in reference⁷ as $\delta_{\text{e}}\text{-Me}$ and $\gamma_{\text{e}}\text{-Me}$ and correspond to the in-plane and out-of-plane methyl bending modes, respectively.

The Raman spectra were recorded from polycrystalline samples in a temperature range between 15 and 280 K using a spectra physics argon laser at 514.5 nm and

a SPEX-Mod. 14018 spectrometer. A sample in a liquid state was poured into a 0.3 cm diameter quartz tube and then cooled. With this procedure very good optical quality of the sample was achieved. The spectra were mostly measured in the energy region between 30 and 200 cm^{-1} , which is the region of the lattice modes and methyl librations. Resolution in this frequency range was 2 cm^{-1} . The resolution profile of the apparatus can be well described by a Gaussian function. Some results of the recorded spectra for both protonated and partially deuterated *p*-xylene are shown in Figures 5a and 5b. These selected spectra show how the shapes of the spectra evolve between 20 K and the ambient temperature. Energies are given with an accuracy of $\pm 1 \text{ cm}^{-1}$. The convolutions of a Gaussian curve, describing the resolution of the apparatus, and a Lorentzian, describing the intrinsic width of the phonon lines, are fitted to the experimental points, giving the energy and the width of the excitations. The solid lines in Figures 5a and 5b indicate the individual contributions of phonons to the spectra.



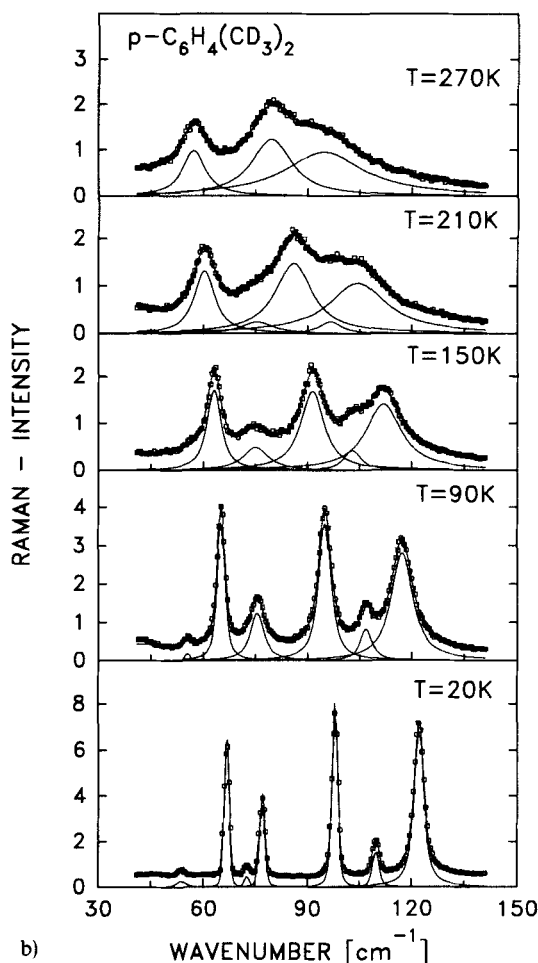


FIGURE 5 a) Raman spectra of protonated *p*-xylene between 20 and 280 K. b) Raman spectra of partially deuterated *p*-xylene between 20 and 270 K. The solid lines are due to the fit procedure described in the text.

The sum of these curves gives the solid line joining the experimental values. The experimental points are well reproduced by this fitting procedure. Note that a linear background, which was also fitted, is not shown in Figures 5a and 5b, for reasons of better transparency in the graphical representation.

The energies of the phonons as well as the full width at half maximum of the Lorentzians are shown in Figures 6a and 6b. Apart from some trivial shifts of excitations at the lowest energies, having their origin in the difference of mass between H and D, the shifts of higher energy excitations show some differences between protonated and partly deuterated *p*-xylene. Calculations shedding some light on this behaviour are given in the next section.

It is quite remarkable, that with increasing temperature the high energy lattice modes especially become very broad, pointing to a large influence of anharmonicity. With

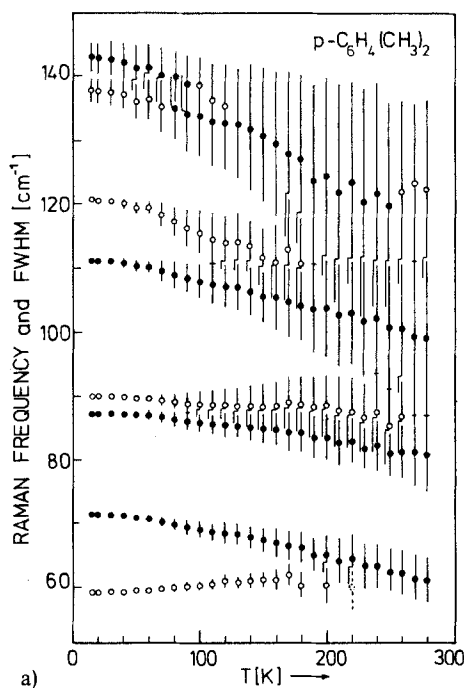
increasing temperature some of the weak excitations are lost, mainly because they become broader and the spectrum fitting quality does not depend on whether they are kept or not. Therefore, we continued the fitting procedure at higher temperatures without accounting for these phonon excitations. Their disappearance then in Figures 6a and 6b is not an indication of a phase transition.

We have observed that the intensity of all phonons increased with increasing temperature, which is to be expected by reasons of the temperature dependence of the Bose population factor. There is one exception: For the strong mode at 143 cm^{-1} ($T = 20\text{ K}$) for protonated *p*-xylene, the opposite behaviour was detected. This might come from some eigenvector mixing with a neighbouring weak phonon line.

P-XYLENE LATTICE DYNAMICS

A harmonic model of the molecular motion of *p*-xylene has been constructed. The main purpose of this calculation was to make an assignment of the observed Raman bands on the bases of the calculated frequencies and symmetry of associated eigenvectors.

In the modelling of molecular crystals it is often not very useful to deal with all 3N Cartesian coordinates of individual atoms. It is usually more economical and clearer to take into account a smaller number of degrees of freedom that are more relevant to the presently considered problem. The most extreme and widely used form of such a reduction in the number of degrees of freedom is the assumption of a completely rigid



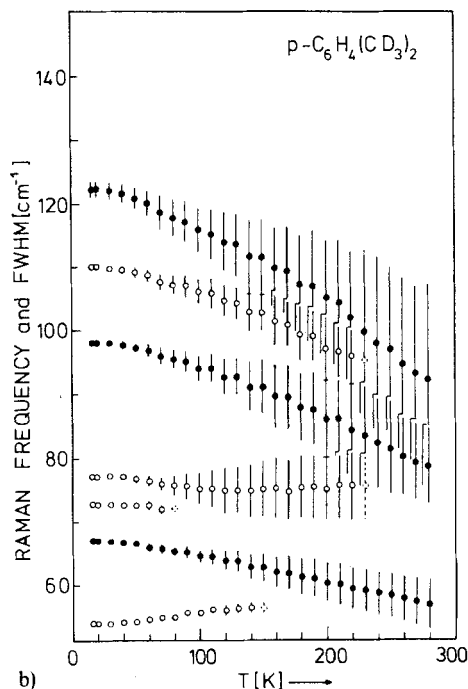


FIGURE 6 a) Temperature dependence of the peak positions of the Raman spectra for protonated *p*-xylene. Open and solid circles indicate weak and strong intensities. The bars indicate the full width at half maximum of the phonon lines, due to the fit procedure explained in the text. b) Same, but for partially deuterated *p*-xylene.

molecule.¹⁷ There are, however, many molecules that cannot be considered as completely rigid. Nevertheless, most of them do contain rigid groups that allow a considerable reduction of the number of relevant coordinates. In general such a semi-rigid molecule may be specified by a number of geometrical constraints, e.g. fixed bond lengths, fixed bond or torsional angles or confinement of atoms to one plane. In the lattice dynamics calculation of *p*-xylene we assumed that all carbon atoms and all hydrogen atoms not belonging to methyl groups built a rigid unit. It is assumed that the hydrogen atoms in the methyl groups, which are rigid units, too, are allowed to perform torsional librations about the C—C bond as the axis.

The potential energy of the crystal may be written as¹⁸

$$V = 1/2 \sum_m \left(k(\varphi_{1m}^2 + \varphi_{2m}^2) + \sum_n V_{mn} \right) \quad (1)$$

where m, n numbers the molecules in the crystal. The first term describes torsions of methyl groups 1 and 2 around the C—C bond as the axis, i.e. the torsional librations of these groups, k is a coupling constant. The last term refers to the interaction between chemically unbound atoms of different molecules and is a superposition of the “6-exp”

functions:

$$V_{mn} = \sum_{ij} A \exp(-B \cdot r_{ij}) - C \cdot r_{ij}^{-6} \quad (2)$$

where r_{ij} is the distance between the interacting atoms. A , B and C are empirical parameters. For the interactions between C—C, C—H and H—H we used a set of parameters (set IVa) proposed by Williams,¹¹ as shown for convenience in Table 2. This set of parameters was found to represent the phonon dispersion curves of benzene very well.¹² No difference in these parameters was made for hydrogen and deuterium.

By a reduction in the number of degrees of freedom, as seen in Equation (1), we have to expect only 16 phonon dispersion curves: three degrees of freedom for translations and librations of the molecule, respectively, and two internal degrees of freedom for the torsional libration of methyl groups. Having two molecules in the unit cell we get the number of dispersion branches mentioned above.

From gas data, it is known that the methyl groups can rotate practically free and therefore, we chose $k = 0$ (see Equation (1)). The large librational frequencies of the methyl groups have their origin in the strong interaction of these groups with atoms of neighbouring molecules.¹⁰ The calculation was performed first by fitting the lattice parameters (these are a , b , c and the angle β as well as the orientation of the molecules and the angular position of the methyl groups) in such a way, that the potential energy of the lattice was minimized. It turned out, that in the mean the lattice parameters a , b , c were 3.54% less than the experimental ones ($a = 0.5484$ nm, $b = 0.4901$ nm, $c = 1.0875$ nm, $\beta = 100.48^\circ$).

It turned out that the calculated phonon frequencies were in mean too large. Therefore we changed the Williams set of parameters to get a better representation of the experimental phonon energies.

A simple way to do this is to multiply only the parameters A and C in Equation (3) by a common factor g in such a way that the phonon energies are better reproduced. The factor g was chosen to be $g = 0.737$. With this correction the phonon energies were reproduced reasonably well but the distance between peaks 2 and 3 in Figures 3 and 4 was a little bit too low. Finally, we changed the interaction energy between the hydrogen (or deuterium) of the methyl groups, by trial and error, in such a way that the distance between peaks 2 and 3 was better reproduced. This was achieved by choosing g to be 0.884 for the interaction between these special atoms. The results of all

TABLE II
Set of parameters of the atom-atom potential functions used for the phonon calculations

Set of potential parameters				
Contact	A/(kcal/mole)	B/(Å ⁻¹)	C/(kcal.Å ⁶ /mole)	Remarks
H—H	2654	3.74	27.3	set of parameters from Williams ¹¹
H—H	8766	3.67	125.0	
C—C	83630	3.60	568.0	

calculations shown in this paper are given by taking into account all of these modifications.

As mentioned above, the values of the calculated lattice parameters a , b and c were less than the experimental ones. To improve this, we changed the set of parameters of Williams in such a way, that a , b and c were reproduced better in the mean. This was done by a very simple transformation in Equation (2) with $r_{ij}(\text{new}) = f \cdot r_{ij}(\text{old})$ with $f = 0.935$, giving

$$V_{mn}(\text{new}) = \sum_{ij} A \cdot \exp(-B \cdot f \cdot r_{ij}) - C(f \cdot r_{ij})^{-6} \quad (3)$$

Then, the calculated lattice parameters have the following values: $a = 0.5646$ nm, $b = 0.5138$ nm, $c = 1.1166$ nm and $\beta = 100.48^\circ$. The values of a , b and c correspond in the mean with those measured in reference¹⁰ but nevertheless show deviations from the measured ones in the range of a few percents. Unfortunately the agreement between calculated and measured phonon energies worsened.

In Table 3 we present the phonon energies at the Γ -point, as calculated. Included in this table are assignments with respect to the character of these modes for protonated and partially deuterated *p*-xylene. The Raman-active modes are assigned by *R* (the displacement patterns of the atoms show an inversion symmetry with respect to the center of gravity of the molecule), whereas the infrared-active modes are assigned by

TABLE III

The calculated phonon frequencies at Γ -point for protonated and partially deuterated *p*-xylene. The experimental data are due to Raman-experiments at 14 K. (The value in parenthesis comes from an IR-measurement at 94 K). In the column "assignment" the character of these modes is indicated. (R = Raman-active, I = infrared-active). The indices indicate approximately the direction of the axes of rotation of the *R*-modes and the displacement vectors for the *I*-modes. The index CH3 means a nearly pure libration of the CH₃-groups. The plus and minus sign is an indication of the phases (in-phase or out-of-phase by π) of the displacement vectors of the atoms in the two molecules in the unit cell with respect to the screw operation of the crystal

Mode No.	C ₆ H ₄ (CH ₃) ₂			C ₆ H ₄ (CD ₃) ₂		
	$\hbar\omega/\text{cm}^{-1}$ exp	$\hbar\omega/\text{cm}^{-1}$ calc	Assignment	$\hbar\omega/\text{cm}^{-1}$ exp	$\hbar\omega/\text{cm}^{-1}$ calc	Assignment
1	-	-	I _a	-	-	-
2	-	-	I _b	-	-	-
3	-	-	I _c	-	-	-
4	-	34.1	I _a (+)	-	32.8	I _a (+)
5	59	56.6	R _z (+)	54	52.7	R _z (+)
6	71.5	58.9	R _x (-)	67	53.0	R _x (-)
7	-	60.5	I _b (-)	-	54.3	I _b (-)
8	87	77.8	R _x (+)	73	70.6	R _x (+)
9	(79)	86.6	I _c (+)	77	77.1	R(-)
10	90	88.6	R(-)	-	83.5	I _c (+)
11	111	117.1	R _y (+)	-	97.4	I _{CD3} (-)
12	121	125.9	R _y (-)	98	100.2	R(+)
13	-	127.3	I _{CH3} (-)	-	100.5	R(+)
14	137.5	134.8	R _x (-)	110	106.0	R _x (-)
15	-	139.3	I _{CH3} (+)	-	121.2	R _x (+)
16	143	145.9	R _x (+)	122.5	123.1	R _x (-)

I (displacement patterns of the atoms show no inversion symmetry with respect to the center of gravity of the molecule). Both kinds of modes are sensitive to inelastic neutron scattering. Included in Table 3 are our results of Raman measurements at 14 K and the most prominent absorption line of an IR experiment⁷ at 96 K.

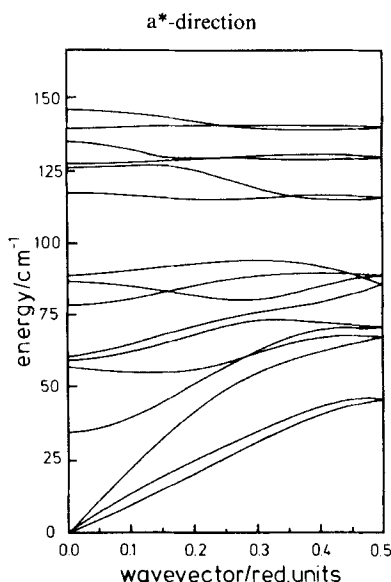
In Figure 7 we present the calculated dispersion curves in the a^* , b^* and c^* directions for protonated p -xylene. In addition we present in Figure 8 the amplitude weighted phonon density of states $G(\omega)$ calculated with the modified set of potential parameters. The results for $G(\omega)$ can be directly compared with the measured IINS-spectra.

Now we will give a more accurate description of the character of the calculated phonon modes for the phonon wavevector $\vec{q} = 0$ (Γ -point) for protonated p -xylene. The two molecules in the unit cell are connected by a 180° rotation around the crystallographic b -axis and a shift of the molecule by 0.5, 0.5, 0.5. With respect to this symmetry operation the phases of the displacement vectors of the atoms are defined as in-phase (indicated by the symbol (+)) and out-of-phase (the phase difference is π and is indicated by the symbol (—)). We introduce an orthogonal x, y, z -coordinate system fixed to the molecules at their center of gravity. x and y lie in the plane of the benzene ring and z is normal to this plane. The x -axis goes through the C-atoms of the methyl groups (see Figure 1) and the y -axis is perpendicular to x .

34.1 cm^{-1} (+): This is a translation of the molecules close to the a -direction. IR-active.

56.6 cm^{-1} (+): This is a libration of the molecule around an axis close to its z -axis. Raman-active. The displacement pattern of this mode is shown in Figure 9a.

58.9 cm^{-1} (—): This is a libration of the molecule nearly around its x -axis. The axis of libration is not confined to the x - y plane of molecule. If the C_6H_{10} -ring librates



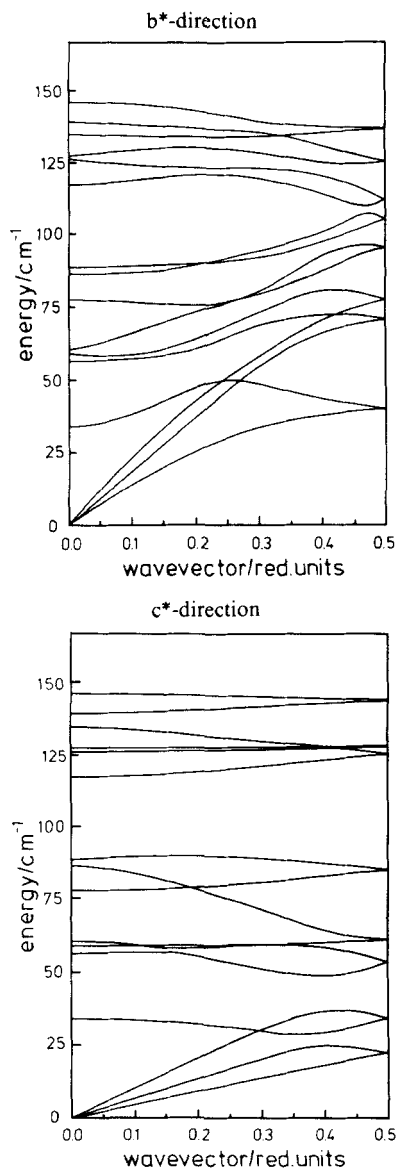


FIGURE 7 The calculated phonon dispersion curves in a^* -, b^* - and c^* -directions for protonated p -xylene with our adapted set of parameters. The wavevectors are given in reduced units.

clockwise, the CH_3 -groups librate anticlockwise and vice versa. Raman-active.
 $60.5 \text{ cm}^{-1}(-)$: This is predominantly a translation of the molecule nearly along the b -axis. For a rigid molecule the translation would be along the b -axis. IR-active.
 $77.8 \text{ cm}^{-1}(+)$: This is a libration mode like the $58.9 \text{ cm}^{-1}(-)$ mode, but the motion of the two molecules is symmetric with respect to the screw operation. Raman-active.

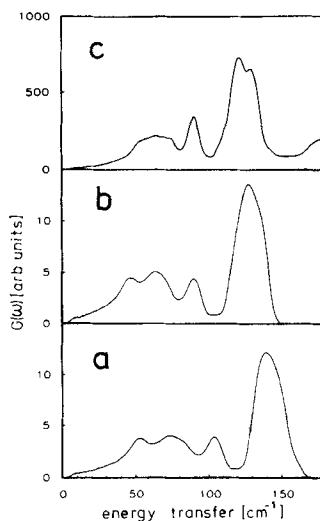


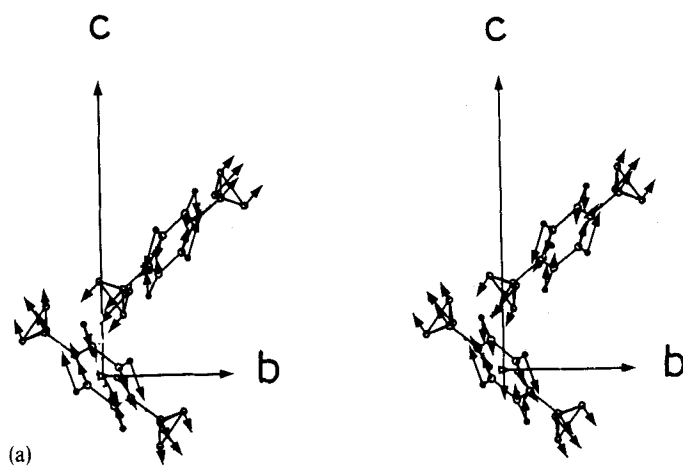
FIGURE 8 The calculated weighted phonon density of states $G(\omega)$ for protonated *p*-xylene (in arbitrary units) using the William set of parameters¹¹ (a) and the modified set of parameters (b) convoluted with the resolution of the NERA spectrometer. The uppermost curve (c) represents experimental results of *p*-xylene at 10 K.

The displacement patterns of this mode are shown in Figure 9b.

$86.6\text{ cm}^{-1}(+)$: This is a translational mode nearly along the c^* -axes. IR-active.

$88.6\text{ cm}^{-1}(-)$: This is a libration around an axis out of the x - y plane of the molecule and being oriented approximately inbetween the x and z -axes. The C_6H_{10} -ring librates in antiphase to the CH_3 -groups. Raman-active.

$117.1\text{ cm}^{-1}(+)$: This is a libration around an axis near the y -axis of the molecule. Raman-active.



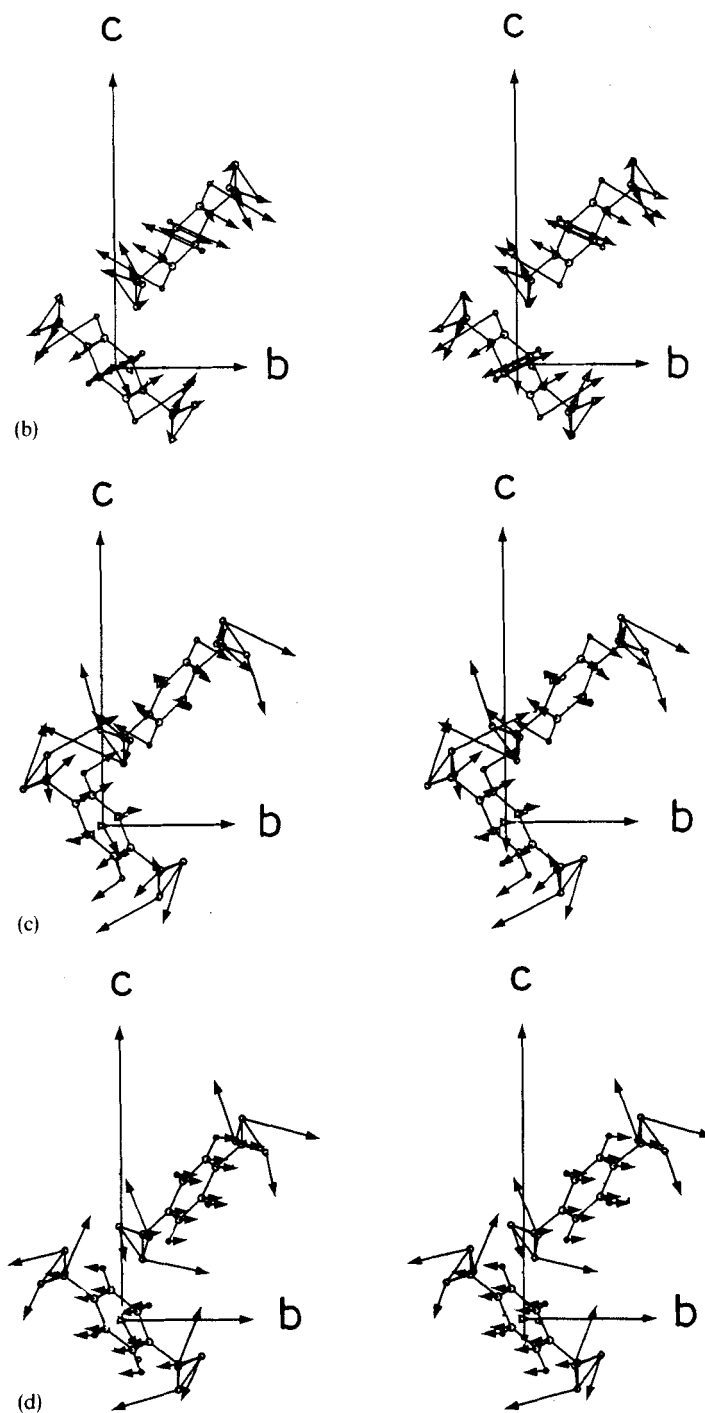


FIGURE 9 The calculated displacement pattern of the 56.6 cm^{-1} mode (a), the 77.8 cm^{-1} mode (b), the 125.9 cm^{-1} mode (c), and the 127.3 cm^{-1} mode (d). Notice, that stereographic views are presented.

$125.9\text{ cm}^{-1}(+)$: This mode is like the $117.1\text{ cm}^{-1}(+)$ mode. The axis is nearly confined to the x - y plane of the molecule and oriented approximately halfway between the x and y directions. The libration of the CH_3 -groups is in the same direction as the libration of the C_6H_{10} -ring. Raman-active. The displacement patterns of this mode are shown in Figure 9c.

$127.3\text{ cm}^{-1}(-)$: This mode shows a strong libration of the CH_3 -groups. The two methyl-groups rotate clock- and anti-clockwise. The C_6H_{10} -ring moves nearly in b -direction and shows no libration. IR-active. The displacement patterns of this mode are shown in Figure 9d.

$134.8\text{ cm}^{-1}(-)$: This is a libration nearly around the x -axis. The motion of the CH_3 -groups are in phase with the libration of the C_6H_4 -ring. Raman-active.

$139.3\text{ cm}^{-1}(+)$: This is a pure libration of the CH_3 -groups, like the $127.3\text{ cm}^{-1}(-)$ mode, but the motion of the two molecules is antisymmetric with respect to the screw operation. IR-active.

$145.9\text{ cm}^{-1}(+)$: This is like the $134.8\text{ cm}^{-1}(-)$ mode, but the motion of the two molecules is symmetric with respect to the screw operation. Raman-active.

According to our calculations we found, that for protonated p -xylene, the six phonon branches, numbered by Nos. 11–16 in Table 3, are responsible for the peak No. 3 of the inelastic neutron spectra in Figures 3 and 4. Two of these branches are infrared-active modes at the Γ -point. The shape and intensity of peaks Nos. 2 and 3 of Figures 3 and 4 are reproduced quite well by our calculation. The peak No. 2 comes into reality from a superposition of phonon branches Nos. 8, 9 and 10 of Table 3 (see Figure 7 for comparison, as well). The energy of the calculated high-energy modes agrees within 10% of the values deduced from the Raman and IR-measurements. The disagreement is larger for two Raman frequencies of the lowest energies (mode 6 and 8). This disagreement between theory and experiment of low energy phonons is also seen in the weighted density of states (see Figure 8). Here, our model is certainly open to some improvements.

We found, for the character of the calculated phonon modes for partially deuterated p -xylene ($\text{C}_6\text{H}_4(\text{CD}_3)_2$), the assignments as shown in Table 3. The orientations of the polarization vectors are not very different from those of $\text{C}_6\text{H}_4(\text{CH}_3)_2$, but the energies, of course, are altered. Again, the energy of one of the Raman-active modes (in this case it is mode No. 6) is not well reproduced by the calculation. The energies of the two uppermost Raman-active modes are according to the calculation nearly equal, supporting the fact that we found experimentally only one Raman-active mode in this energy range, being broader than expected from the energy resolution of the Raman apparatus (see Figure 5b, 20 K). In general, the agreement between experiment and theory is better than for the non-deuterated p -xylene.

THE TEMPERATURE DEPENDENCE OF THE RAMAN-ACTIVE MODES

For both the Raman-active modes (see Figures 5 and 6), as well as for the amplitude weighted phonon density of states $G(\omega)$ (see Figure 4 and Table 1), we observe a substantial increase in mode frequencies with decreasing temperature. There are only a few exceptions to this trend, related to the lowest Raman-active modes in both protonated and partially deuterated p -xylene, which show the opposite behaviour.

Two effects are responsible for the temperature dependence of the mode frequencies. One contribution stems from thermal expansion of the lattice cell volume $\Delta(V(T))$ and the other from the shift associated with anharmonicity caused by the increase in amplitude of the atomic motion with temperature $\Delta(T)$. The combination of these effects gives mode frequencies of:

$$\nu(T) \approx \nu(0) + \Delta(T) + \Delta(V(T)) \quad (4)$$

where $\Delta(V(T))$ can be approximated (see ref. 19) and is given by

$$\Delta(V(T)) \approx \nu(0)((V(0)/V(T))^\gamma - 1) \quad (5)$$

where γ is the mode Grüneisen parameter. Unfortunately these Grüneisen parameters are not available, whereas $V(T)$ is known in the temperature range between 4 and 270 K^{9,10} (see Figure 2).

$\Delta(V(T))$ decreases with increasing temperature, provided $\gamma > 0$, which is normally true. $\Delta(T)$ can increase or decrease with increasing temperature, depending on anharmonic force constants. The observed increase in frequency with increasing temperature of some Raman modes can have its origin in a negative value of γ and a positive anharmonic contribution. For naphthalene¹⁹ and anthracene²⁰ experimental values of mode Grüneisen parameters γ are available. The values of γ for these molecular crystals are in a range of approximately 3 to 5. Taking these values as a guide, we can speculate, that $\Delta(V(T = 250 \text{ K}))/\nu(T = 0 \text{ K})$ is somewhere between -17% for $\gamma = 3$ and -27% for $\gamma = 5$ for *p*-xylene. The energy decrease between 12 K and 250 K for most of the Raman modes (see Figure 6) is even lower than the value of -17% . This suggests that the anharmonic part $\Delta(T)$ is positive for most of the modes. Such a behaviour is not unusual, as the calculations for naphthalene have shown.²¹

The linewidth becomes extremely large for the highest Raman modes. The widths are not always linear in temperature (see Figure 10), which points to the influence of higher than cubic terms in the expansion of the potential energy of Equation (2) with respect to small deviations of atoms from their mean positions. The cubic terms alone will give a linewidth proportional to T at high temperature and some finite linewidth at $T \rightarrow 0$.²¹ We mention here that even for $T \rightarrow 0$ a linewidth of the highest Raman modes was observed (see Figure 6). For these modes the libration of the CH_3 - and CD_3 -groups is large. Therefore, it is evident that anharmonicity for these kinds of modes plays an essential role. Normally, one can assume that for CD_3 -groups the influence of anharmonicity is less than for CH_3 -groups. This stems from the fact that at the same temperature the amplitudes of the CD_3 -librations are reduced in comparison to the CH_3 -librations. Experimentally, we observed this behaviour. (We mention here, again, that the highest Raman line in partially deuterated *p*-xylene is an unresolved doublet, as indicated by the lattice dynamics calculation).

SUMMARY

We have shown that a simple and small modification of a well-established set of parameters for an interaction potential between atoms of different molecules can describe reasonably well the lattice dynamics of a molecular crystal, even in the

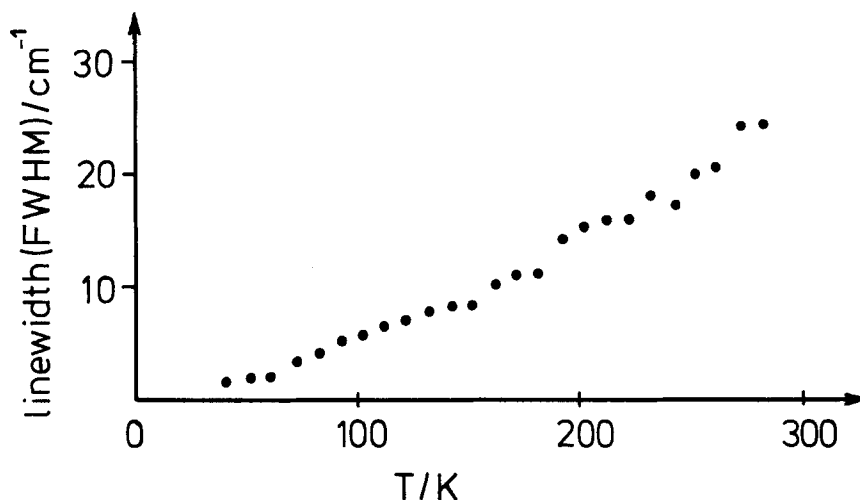


FIGURE 10 Temperature dependence of the linewidth (FWHM) of the 111 cm^{-1} mode (14 K) of protonated *p*-xylene.

presence of freely rotating methyl groups (in the gas phase). It seems that the presence of methyl groups weakens the interaction between molecules, compared to situations in molecular crystals without such groups, with the probable exception of hydrogen contacts between neighbouring methyl-groups.

Acknowledgements

We thank the KFA Jülich and the Joint Institute for Nuclear Research, Dubna, for providing the neutron facilities. Financial support from the Bundesministerium für Technologie under Grant No. 03-KA3BAY-7 is gratefully acknowledged.

References

1. D. G. Lister, J. N. McDonald and N. L. Owen, *Internal Rotation and Inversion*, Academic Press, London (1978).
2. D. Cavagnat, J. Lascombe, J. C. Lassegues, A. J. Horsewill, A. Heideman and B. J. Suck, *J. Physique* **45**, 97 (1984).
3. M. Prager, R. Hempelmann, H. Langen and W. Müller-Warmuth, *J. Phys.: Condens. Matter* **2**, 8625 (1990).
4. A. M. I. Ahmed, G. R. Eades, T. A. Jones and J. P. Llewellyn, *J. Chem. Soc. Faraday Trans.* **68**, 1316 (1972).
5. H. Langen, A. -S. Montjoie, W. Müller-Warmuth and H. Stiller, *Zeitschr. Naturforschung* **42a**, 1266 (1987).
6. S. Julien-Laferriere and J. M. Lebas, *Spectrochimica Acta*, **27 A**, 1337 (1971).
7. S. Julien-Laferriere and J. M. Lebas, *C. R. Acad. Sc. Paris*, **B 272**, 224 (1971).
8. N. V. Sidorov, *Zh. Prikl. Spektrosk.* **40**, 119 (1984).
9. H. van Koningsveld, A. J. van der Berg, J. C. Jansen and R. de Goede, *Acta Cryst.* **B 42**, 491 (1986).
10. M. Prager, W. I. F. David and R. M. Ibberson, *J. Chem. Phys.* **95**, 2473 (1991).
11. D. E. Williams, *J. Chem. Phys.* **47**, 4680 (1976).
12. G. Taddei, H. Bonadeo, M. P. Marzocchi and S. Califano, *J. Chem. Phys.* **58**, 966 (1973).

13. G. Baluka, A. V. Belushkin, S. I. Bragin, T. Zaleski, M. Z. Ishmukhametov, I. Natkaniec, W. Olejarczyk and J. Pawelczyk, JINR Communication P13-84-242, Dubna (1984).
14. I. Natkaniec, S. I. Bragin, J. Brankowski and J. Mayer, Proceedings of ICANS-XII, RAL, Abington, May 24–28 (1993).
15. E. L. Bokhenkov, I. Natkaniec and E. F. Sheka, *Sov. Phys. JETP* **34**, 536 (1976).
16. J. Kalus, J. Wolfrum, F. Wörlen, K. Holderna-Natkaniec, I. Natkaniec, M. Monkenbusch and M. Prager, Phonon Scattering in Condensed Matter VII; Ed. by M. Meissner and R. O. Pohl; Springer-Verlag Berlin, Heidelberg, p. 521–523, 1993.
17. G. S. Pawley, *Phys. stat. sol.* **20**, 347 (1967).
18. M. Monkenbusch, *A Procedure for the Automatic Choice of Dynamical Coordinates for Semirigid Molecules*, Jülich report 1986.
19. U. Schmelzer, E. L. Bokhenkov, B. Dorner, J. Kalus, G. A. Mackenzie, I. Natkaniec, G. S. Pawley and E. F. Sheka, *J. Phys. C: Solid State Phys.* **14**, 1025–1041 (1981).
20. W. Häfner and W. Kiefer, *J. Chem. Phys.* **86**, 4582–4596 (1987).
21. V. K. Jindal and J. Kalus, *J. Phys. C: Solid State Phys.* **16**, 3061–3080 (1983).
22. J. Kalus, *Journal de chimie physique* **82**, 137–152 (1985).